Product Screening of Fast Reactions in IR-Laser-Heated Liquid Water Filaments in a Vacuum by Mass Spectrometry†

A. Charvat,‡ B. Stasicki,§ and B. Abel*,‡

Institut für Physikalische Chemie der Universität Göttingen, Tammannstrasse 6, D-37077 Göttingen, Germany, Max-Planck-Institut für biophysikalische Chemie, Am Fassberg 11, D-37077 Göttingen, Germany, and DLR, Institut für Aerodynamik und Strömungstechnik, Bunsenstrasse 10, 37073 Göttingen, Germany

Received: September 13, 2005; In Final Form: January 11, 2006

In the present article a novel approach for rapid product screening of fast reactions in IR-laser-heated liquid microbeams in a vacuum is highlighted. From absorbed energies, a shock wave analysis, high-speed laser stroboscopy, and thermodynamic data of high-temperature water the enthalpy, temperature, density, pressure, and the reaction time window for the hot water filament could be characterized. The experimental conditions (30 kbar, 1750 K, density ∼1 g/cm^3) present during the lifetime of the filament (20−30 ns) were extreme and provided a unique environment for high-temperature water chemistry. For the probe of the reaction products liquid beam desorption mass spectrometry was employed. A decisive feature of the technique is that ionic species, as well as neutral products and intermediates may be detected (neutrals as protonated aggregates) via time-of-flight mass spectrometry without any additional ionization laser. After the explosive disintegration of the superheated beam, high-temperature water reactions are efficiently quenched via expansion and evaporative cooling. For first exploratory experiments for chemistry in ultrahigh-temperature, -pressure and -density water, we have chosen resorcinol as a benchmark system, simple enough and well studied in high-temperature water environments much below 1000 K. Contrary to oxidation reactions usually present under less extreme and dense supercritical conditions, we have observed hydration and little H-atom abstraction during the narrow time window of the experiment. Small amounts of radicals but no ionic intermediates other than simple proton adducts were detected. The experimental findings are discussed in terms of the energetic and dense environment and the small time window for reaction, and they provide firm evidence for additional thermal reaction channels in extreme molecular environments.

1. Introduction

Chemistry at extreme conditions, i.e., temperature, pressure, and density, is of fundamental interest because experimental data in exotic molecular environments are providing some nonintuitive results that are challenging tests for theories.[1] The drive to model the chemistry in flames, in other combustion systems, and in high-enthalpy air flows has motivated many studies of chemistry at high temperatures and pressures. Many studies of elementary processes under these conditions have been performed in shock tubes, typically at temperatures in the range 1000−2000 K.[2] Although, high-pressure and high-temperature gas phase systems are often complex, systems in the condensed phase or at liquid phase densities are even more challenging and have a large potential for technical applications. Novel methods are being employed to examine chemistry in the condensed phase at extremely high temperatures and pressures. For example, Suslick and co-workers use ultrasound to initiate sonochemistry. In their work, ultrasound is directed into a liquid creating bubbles that grow and then implosively collapse.[3,4] Studies of chemical dynamics in gem anvil cells are beginning to be carried out and some unique chemical synthesis can also occur at these extreme conditions.[2] Dlott and co-workers have developed a technique to generate shock waves with fast rise times in specially designed assemblies, which are then probed spectroscopically with picosecond time resolution.[5] Recently, the groups of Baer and Miller have developed a technique for laser heating of liquid aerosol droplets with subsequent mass analysis of the reaction products.[6−10] Laser-initiated decomposition of single aerosol particles in the source region of a time-of-flight spectrometer, followed by vacuum ultraviolet laser ionization and mass analysis of the reaction products, revealed the identity of species formed in the early stages of condensed-phase decomposition of several molecules embedded in the droplet.

Chemistry in supercritical fluids, for example, is drawing increasing attention for the possibility of replacing organic solvents in synthetic, purification, and separation processes.[11] Of the many solvents available for chemistry water is still special (T_c = 647 K, p_c = 221 bar, ρ_c = 322 kg/m^3). A number of reviews have looked at reactions in supercritical water.[12−16] Studies of energy transfer in competition to chemical reaction in supercritical fluids provide an important way to bridge our understanding of dynamics in the gas phase and liquid phase.[16,17] Often gas-phase combustion rate constants are used to model reactions in high-temperature water.[18] Kinetic models based upon these rate constants often fail particularly at higher water densities, even when they are corrected for high pressures, in part because the models do not account for solvation effects[16] and ionic mechanisms.[14,19,20]

† Part of the special issue "Jürgen Troe Festschrift".

* Corresponding author. E-mail: BABEL@GWDG.DE.

‡ Institut für Physikalische Chemie der Universität Göttingen and Max-Planck-Institut für biophysikalische Chemie.

§ Institut für Aerodynamik und Strömungstechnik.

10.1021/jp055165e CCC: $33.50
Published on Web 02/10/2006

Most of the mechanistic knowledge about reactions at high-temperature conditions has been obtained from off-line chemical analysis following conversion in a batch or flow reactor. Dynamic, real-time analysis, however, has a higher potential to deepen insight into the details and mechanisms of high-temperature water reactions.[21] Unfortunately, direct and selective (time resolved) in situ spectroscopic measurements are often difficult due to spectral overlap and often unknown spectra of many transient species, intermediates and product molecules. A variety of readily available spectral methods such as IR,[21] Raman,[22,23] and electronic spectroscopy[24,25] are being used to characterize reactions at high-temperature conditions, each of them having its strengths and weaknesses. A practical aspect of high temperature and supercritical water investigations is the fact that water at these conditions reacts with most materials commonly used to construct reaction as well as spectroscopic cells.

In the present contribution we present an alternative novel analytical approach that is similar in spirit to the technique developed by Baer and Miller[6] and is also related to some extent to the LILBID[26] and IR-MALDI[27] processes. We use a pulsed IR laser tuned in resonance with the OH-stretch absorption of bulk water for rapid and extreme heating of a 10−12 μm diameter water filament in a vacuum,[28] which in turn disintegrates after some time. In this process, reactants, products and reaction intermediates are isolated and energetically quenched in the gas phase. A fraction of the neutrals are protonated and may be analyzed together with real ions via subsequent mass spectrometry.[29,30] Because the technique does not involve an ionizing laser for the ionization process, the technique relies upon preformed ions or ionic aggregates that are not neutralized due to charge recombination in the desorption process. It should be noted here that the detection of protonated species provides a quantitative measure of neutrals in the condensed phase with a linear response of the gas-phase signal on the solution phase concentration of neutrals, as has been shown recently.[31]

In the present article we report first results on new reaction pathways of resorcinol in extremely heated water at very high pressure and liquid water density. The high-temperature kinetics of phenols and substituted phenols have been studied by several groups because of their role as model pollutants.[12,14,32−36] Typically, phenol and resorcinol in supercritical (SC) water undergo oxidation reactions on longer time scales induced by OH radicals.[14] Products of phenol and resorcinol oxidation in SC water include dimers (e.g., phenoxyphenols, biphenols, dibenzofuran) single-ring compounds, ring-opening products such as carboxylic acids and finally CO_2.[14] Our intention was to set up a device that is able to quickly screen and identify ionic and neutral intermediates or products of fast decomposition reactions in a particular time window in water under extreme conditions and to look for new chemistry under these extreme conditions.

2. Experimental Section

A. Experimental Approach. We employed a thin water beam (12−13 μm diameter, flow speed 40 m s^{-1}) containing the compounds under investigation, which is ejected into the vacuum chamber at high pressure (see Figure 1). The liquid jet is rapidly heated in the focus of an IR laser pulse tuned in resonance with the OH-stretch absorption of bulk water[29] to produce superheated (supercritical) water at high density (∼1 g/cm^3) for about 30 ns before the hot beam expands and disintegrates. As the heating rate achieved in our experiments is extraordinarily high (on the order of 10^{11} K s^{-1}), the critical temperature of water T_c = 647 K can, in principle, be already reached early in the leading edge of the laser pulse. Indeed, numerical estimations show that only a small fraction of the total available energy is sufficient to raise the temperature up to the critical one such that the filament is heated much beyond T_c. It should be emphasized here that the laser energy is controlled in a way that plasma formation is avoided and not an issue here. The choice of the wavelength of λ = 2695 nm (see Figure 2a) is a tradeoff between a large penetration depth that ensures a relatively homogeneous heating of the irradiated beam volume segment and the overall absorption that should be optimized. The absorbed energy of the IR laser is redistributed within picoseconds[37−39] and heats the volume to a high but initially unknown temperature. The time scale for supercritical water reactions in the filament between the excitation process and the unavoidable explosive beam disintegration, which efficiently quenches reactions, has been characterized via high-speed laser stroboscopy.[40] Although the enthalpy of the high-density supercritical state of water could be determined from accurate measurements of the absorbed IR laser energy, the initial high pressure of the supercritical water filament could be estimated from thermodynamics and shock wave velocities in air at 1 bar, also recorded with high-speed laser stroboscopy.[40] From our data and thermodynamic data of high-temperature water in the literature we were able to characterize the temperature, density, pressure, as well as the reaction time window of the hot water filament.

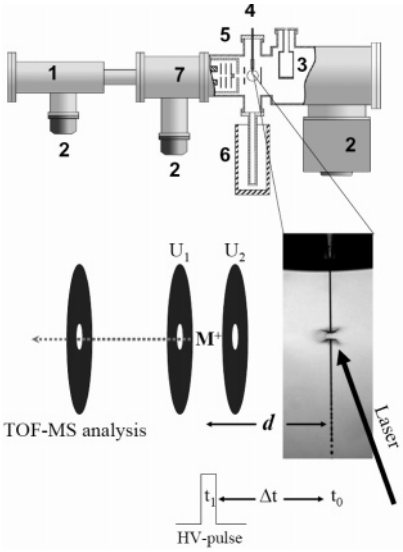

Figure 1. Experimental setup and details of the liquid beam ion source: 1, reflectron time-of-flight mass spectrometer; 2, turbo pump; 3, liquid nitrogen cryo-trap; 4, nozzle with *x*,*y*,*z*-manipulator; 5, ion optics; 6, cryo-trap for the liquid beam; 7, differential pumping stage; U1,U2, accelerating voltages of the ion optics; d, distance between desorption and ion gate; Δt, time between desorption and trigger of the ion optics. The length of the HV-trigger pulse is ∼2 μs.

After the laser-induced temperature jump, an explosive expansion follows after about 30 ns, which accelerates water vapor as well as protonated molecules or ions in free form or within water aggregates of various size ("nanodroplets") that boil off water and stabilize. In the explosive decay of the superheated beam, high-temperature water reactions are efficiently quenched via expansion and evaporative cooling, and reaction products in the form of completely desolvated ionic or protonated species or clusters of various size are finally detected quantitatively via time-of-flight mass spectrometry (TOF-MS) without the need for any additional post-desorption ionization laser. The linearity of the present detection for a large number of molecules is discussed in ref 31. Beyond the multiplex

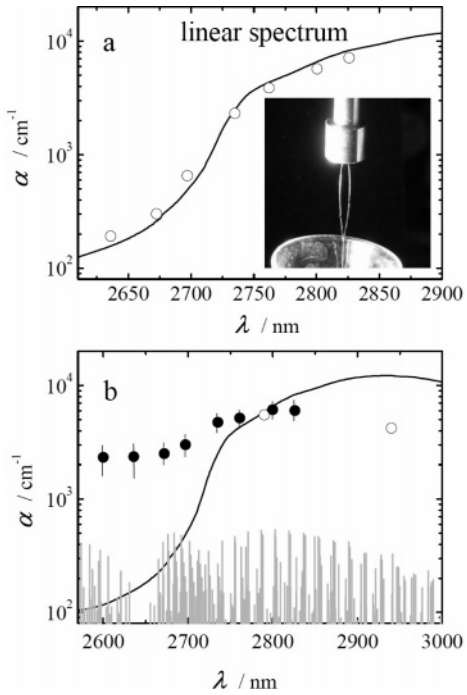

Figure 2. (a) Absorption coefficients α of water in the near-infrared spectral range.[45] ○: absorption coefficient measured with an unfocused IR OPO beam for the determination of the thickness of the center of the planar water jet. In the inset the flat (10 mm long lamellar) water jet with a thickness of 6 μm together with the nozzle head and beam dump is displayed. (b) Absorption coefficients and spectrum of high-temperature water (~1750 K) for the IR-laser-heated water jet measured with a pulsed OPO. The two open circles correspond to two measurements reported in ref 46 for similar conditions. The gray spectrum is a calculated HITRAN gas-phase stick spectrum of water for 1750 K for comparison.

advantage for measuring all reaction products at the same time, the use of a free water jet has a big advantage in terms of the problems outlined above that accompany experiments in static high-pressure cells containing supercritical water.[41]

Because the present technique employs a single laser for initiation of high-temperature chemistry in water and the desorption of organic molecules and fragments at the same time it is related to the LILBID technique[26] and the liquid beam desorption technique employed in our laboratory[31] for the analysis of biomolecules. One may ask the question, why is the technique apparently soft to biomolecules and why does it induce high-temperature chemistry in the present experiment? The main difference of the two applications is the wavelength and the penetration depth of the desorption laser. In the case of the biomolecule desorption, we choose a small penetration depth and disperse the beam with a strong shock wave in the liquid. In this case the liquid beam is irradiated from the back and we collect the desorbed molecules from the front ("lower temperature") side. In this desorption process the biomolecules hardly suffer from a large heat load during desorption. In the present case a uniform and strong heating is desired to obtain a superheated water filament in which high-temperature reactions can take place. Nevertheless, it has also been found that under such conditions large biopolymers can be desorbed without significant fragmentation. This is not in contradiction with the present experiment because the lifetime of the filament as well as the desorption is in general too short for significant fragmentation of large and complex molecules. At the same time the molecules are stabilized through expansion and evaporative cooling. Moreover, large biomolecules have a very large number of internal degrees of freedom, such that even for very large temperatures (as observed here) the molecules do not fragment before they hit the detector of the spectrometer. This may be different for small molecules such as investigated here. Hydration reactions such as seen in the present study cannot be observed for large systems due to a limited and insufficient mass resolution.

B. Experimental Setup. Figure 1 shows the experimental apparatus and a detail of the employed setup. The main components of the experiment consisted of a liquid beam, an IR laser system, and a reflectron time-of-flight mass spectrometer (Kaesdorf).[29] A continuous liquid beam was injected vertically into a vacuum chamber through a quartz nozzle with an inner diameter of 15 μm, forming a water beam with a diameter of about 12 μm. The temperature controlled liquid water was pumped through a sequence of filters and finally through the nozzle at 10 bar with a high-pressure liquid chromatography pump (Gynkotek, Model 300C). The flow rate was kept constant at 0.3 mL/min throughout the experiment. A solution of resorcinol in pure water at a concentration of 0.01 mol/L (M) was employed in the present studies. The liquid beam was trapped in a cold trap about 20 cm downstream from the nozzle (Figure 1). The main chamber was evacuated down to 5×10^{-5} mbar by a 3700 L/s diffusion pump and an additional cryotrap. Traveling a distance of 1−2 mm from the quartz nozzle exit, the liquid beam was crossed with a tightly focused IR laser beam. The IR laser system with output energies between 0.5 and 0.8 mJ/pulse was described in detail in ref 42. For their detection small fractions of the charged species or aggregates are sampled within a small solid angle through a skimmer (field-free space), which is the entrance to the mass spectrometer. The pulsed ion optics of the spectrometer is used here for the acceleration of the molecules for further mass analysis, and most importantly, it acts as a gate for the incoming ionic aggregates. Varying the time Δt, i.e., the time between IR-laser pulse and trigger of the ion optics, allows us to monitor different fractions of molecules from the time dependent desorption process. The main advantage of gating the velocity distribution, however, is the improvement of the mass resolution.[29] The signals were amplified, visualized with a 200 MHz digital oscilloscope (Tektronix), and recorded with a 150 MHz digitizer card (Acqiris) in a computer operated under the LABVIEW software. A Stanford Research Systems DG535 digital delay generator controlled the timing of (the IR laser and) the ion optics. The mass resolution $m/\Delta m$ of the experiment was usually on the order of 1000 in the mass range below 1000 amu. Resorcinol was purchased from Aldrich and used without further purification.

The fast flowing microfilament has been visualized with a high-speed video stroboscope system and a laser illumination technique described in ref 40. Speckle free illumination has been achieved with Rhodamine dye fluorescence from a small dye cuvette (quartz) excited with the second harmonic of a Nd:YAG laser (Indy series, Spectra Physics). These light pulses have been synchronized with the shutter circuit of the stroboscope camera and the IR−Laser pulses. A continuously changing phase shift between the IR−Laser pulses and the shutter opening has been introduced.

3. Results and Discussion

A. OH-Stretch Mode as a Probe of Hydrogen-Bond Structure of High-Temperature Water. Formation of a hydrogen bond O−H:::Y causes a red shift of the fundamental frequency of the OH-stretch (ν_{OH}) vibration. This red shift increases approximately linearly with decreasing hydrogen-bond

distance $R_{O-H:::Y}$. For moderately strong O−H:::Y hydrogen bonds, such as occur in water and ethanol, the red shift of ν_{OH} is typically 200−300 cm^{-1}.[43] Simultaneously, with the red shift of the OH-stretch frequency, an increase of both the line width and the absorption cross section of the fundamental ν_{OH} (0←1) transition occurs for bulk water. The strong correlation of the hydrogen-bond strength and the ν_{OH} frequency has made infrared spectroscopy by far the most important tool to study hydrogen bonding.[43] Therefore, it appears reasonable to use IR spectroscopy for the investigation of the hydrogen bond network in high-temperature water and to verify spectroscopically the high-temperature state of water. We have scanned the wavelength of our infrared system and determined the transmission and the absorbed energy of a focused 0.6 mJ IR pulse in a specially designed flat lamellar microjet (Figure 2a, in the inset) with a thickness of 6 μm. Such jets are otherwise used as ultrathin saturable absorber jets in femtosecond dye lasers in our laboratory.[44] The thickness of the jet in the center was determined to be 6 μm from absorption measurements with an unfocused IR source and the known absorption coefficient of water at 300 K (see Figure 2a). The absorption and the absorption coefficient of water under high-temperature conditions comparable with those of the present experiment were measured with the tightly focused IR laser pulses. In this experiment the IR laser pulse is used for heating the medium and for absorption measurements at the same time. We had to use this extra setup because quantitative measurements with a microjet are difficult due to the thickness of the beam (12 μm) and the unfavorable overlap of the laser beam (80 μm) and liquid jet (12 μm). The normalized absorption coefficients for conditions comparable to those in the experiment are displayed in Figure 2b. The solid line (as in Figure 2a) is the linear absorption coefficient of bulk water at 300 K taken from literature.[45] The filled circles are our absorption measurements. We also included two measurements reported by Vogel et al.[46] (open circles) for comparable conditions. The gray stick spectrum is a high-temperature spectrum for gas-phase water at 1700 K from the HITRAN database. The experimental "spectrum" (●) in Figure 2b suggests that the water hydrogen bond network after laser heating is very loose such that the maximum of the absorption is close to the value for free OH in the gas phase.[43] The observed shift of the measured spectrum as opposed to the bulk spectrum is on the order of 200 cm^{-1}, which may suggest that in the present case the temperature of the water filament is actually very high, very likely above the supercritical temperature.[47] At the same time the measurements clearly show a pronounced decrease of the peak absorption for the fundamental transition but no pronounced narrowing of the band is observable, which is characteristic for free OH of water in the gas phase. However, the latter observation we attribute to the high-pressure and high-density medium causing a strong overall broadening. If we assume that the structure in the HITRAN spectrum is lost because of strong broadening such that only the envelope remains, a similarity with the measured high-temperature spectrum appears obvious. We take the broad shifted absorption feature observed in the present experiment as a first indication for the presence of a dense and very hot phase of water, which will be further characterized in section B.

B. Enthalpy, Pressure, Temperature, and Lifetime of the Hot Filament. Typical pulse energies of our IR laser system are between 0.5 and 0.8 mJ/pulse for a pulse length of 7 ns (fwhm). In the experiments the laser pulse is focused to a focal spot of ∼80 μm (1.6 times D_c, assuming a *Gaussian* profile), as has been measured with the *knife edge* technique (see Figure 3).[48,49] The size of the focus is still significantly larger than the water filament size. The wavelength of interest in our present experiment is 2695 nm, a good compromise between a sufficiently large penetration depth for homogeneous heating and high absorption enabling us to couple enough energy into the water filament. To use the present method of laser-heated water for high-temperature kinetic investigations, the conditions of the high-temperature water environment have to be determined as precisely as possible. It is simple to show that the energy input is sufficient to completely evaporate the water jet, as seen in a series of micrographs of the exploding beam in Figure 4. For a 12−13 μm diameter jet and a laser focus of 80 μm the laser pulse is absorbed in a volume of approximately 1×10^{-8} cm^3. If we neglect laser light scattering for a moment, about one-fifth of the pulse strikes the jet such that we have ∼0.14 mJ for a 0.7 mJ pulse. The energy required to completely evaporate this volume of water is about 20 μJ—so that the laser

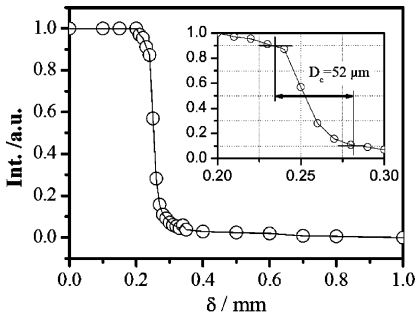

Figure 3. Knife edge measurements for the determination of the focus diameter and the intensity in the focus of the laser beam used for the absorption measurements and the laser-induced heating of the water filament. The beam diameter ($1/e^2$ intensity decay) for a *Gaussian* profile is in this case $1.56D_c = 80$ μm. In the inset an enlarged range is displayed.

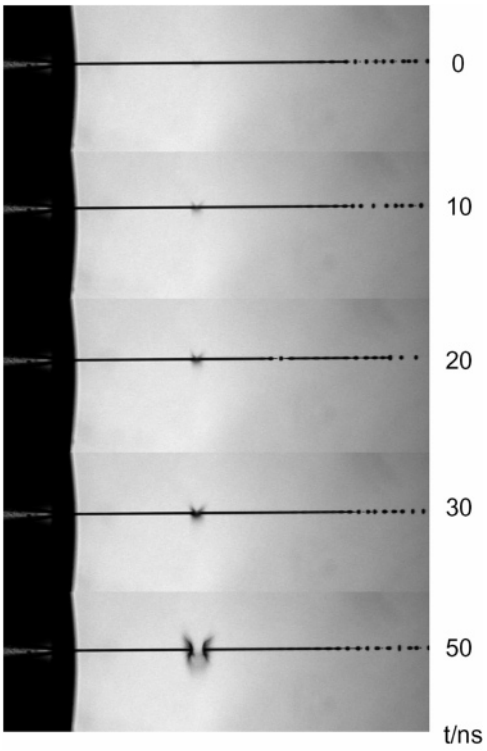

Figure 4. Series of high-speed pictures that display the time for disintegration of the hot (supercritical) volume of the laser-heated water beam after laser impact explosion taken with the stroboscope technique described in the text. The time of the particular time sequence is given as well.

pulse energy is about 7 times that needed. If we take into account scattering of 3 μm light on a small cylindrical object with dimensions on the order of the laser wavelength, the laser energy that can be coupled into the water beam is reduced by about 50%.[50] The enthalpy (i.e., the energy content) of the heated filament as determined from the absorbed energy (0.7 mJ pulse) for this case is 127 kJ/mol. Interestingly, this energy content is comparable with that of many conventional explosives.[51] Because the enthalpy alone is not sufficient to determine the temperature, density, and pressure in the filament precisely (it depends on T and p), we have first estimated the pressure in the filament from thermodynamics. In general, the pressure change (of a fluid) due to a change in temperature and volume is given as

$$\mathrm{d}p = \left(\frac{\partial p}{\partial T}\right)_V \mathrm{d}T + \left(\frac{\partial p}{\partial V}\right)_T \mathrm{d}V = B_T\beta\,\mathrm{d}T - \frac{B_T}{V}\mathrm{d}V = B_T\beta\,\mathrm{d}T + \frac{B_T}{\rho}\mathrm{d}\rho \quad (1)$$

with B_T being the isothermal bulk modulus and β the isobaric volume expansion coefficient.[52] Simple estimates of the magnitude of the pressure are possible in the stress confinement regime.[46,53,54] From eq 1 we obtain for $\mathrm{d}V = 0$ and constant density ρ,

$$\Delta p = B_T\beta\Delta T = \frac{B_T\beta}{\rho c_V}\epsilon = \beta\frac{c_S^{\,2}}{c_V}\epsilon = \Gamma\epsilon \quad (2)$$

where ϵ is the energy density of the excited volume, c_S is the sound velocity in bulk water, c_V is the specific heat, and Γ is the *Grüneisen* parameter[54] for bulk water that provides a measure for the efficiency of converting energy into pressure. For a given energy density calculated from the absorbed energy in the filament volume and the dimensionless Grüneisen parameter at the highest temperature, which is known from literature (Γ(600 K) = 0.34),[46] we calculated a pressure of 25 $\pm$ 5 kbar, and from the specific heat of water at high temperatures,[53,55−58] we estimate a temperature jump of 1500−2000 K. Due to the lack of high-temperature data (parameters in eq 2), the above estimates, however, may not be very accurate, such that it would be advantageous to have an additional independent (and more accurate) method.

To measure the pressure in the hot superheated water filament more directly, we have monitored micro shock waves in air that originate from the irradiated microjet for the same internal energy as detailed above (Figure 5). The increasing radius of the shock wave (SFR) is plotted against time, and an expression $\mathrm{SFR}(t) = A(E)t^x$, with $A = 8.5 \pm 1.1$ and $x = 0.67 \pm 0.01$, is fitted to the data (Figure 6).[59,60] From these data an initial shock wave velocity can be determined to be close to 2000 m s^{-1}. It has been shown that strong shock waves enable the determination of the equation of state (EOS) of water for extreme temperatures and pressures. Rice and Walsh[61] have measured the EOS of water up to 250 kbar in water shock wave experiments. They have also investigated water/air interfaces at which shocks were reflected, creating a large pressure p and an interface particle velocity that compresses air at the interface creating a shock wave in air.[62] The water/air interface velocity was given by Rice and Walsh as a function of initial water (shock) pressure,[61] which is plotted in Figure 7 (upper panel). From these data we determine a filament pressure of 30 $\pm$ 5 kbar. From high-enthalpy data given in ref 63 for 30 kbar (Figure 7, lower panel) we are able to determine a temperature

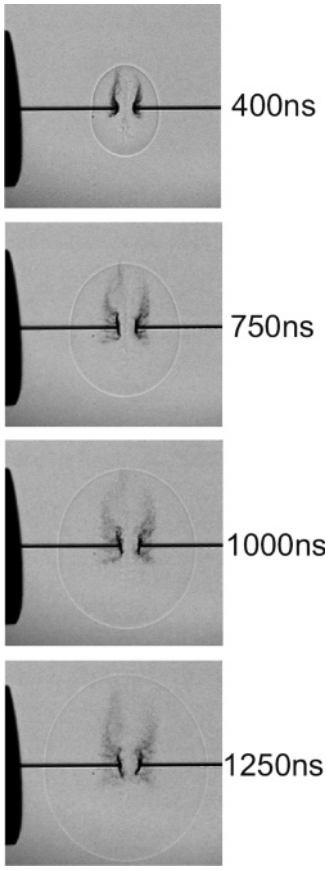

Figure 5. High-speed pictures display the formation and propagation of a shock wave in air recorded with the stroboscope technique. The laser is approaching from the top.

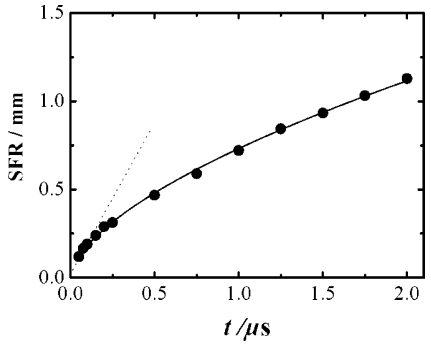

Figure 6. Radius of a shock front (SFR) as a function of time. The solid line displays a fit through the experimental data. For details see the text.

of 1750 $\pm$ 190 K for the water filament for a 0.7 mJ IR laser pulse. This result corresponds to a *Grüneisen* parameter of 0.3,[46,54] in fair agreement with the previous estimate. With this somewhat involved but nevertheless powerful approach we are able to determine the temperature and pressure of the high-temperature water filament. The determined experimental conditions (30 kbar, 1750 K, density $\sim$1 g/cm^3) are indeed rather extreme and unique and provide an interesting environment for high-temperature water chemistry on short time scales.

For quantitative kinetic measurements it is important to know for how long these conditions remain nearly unchanged. In Figure 4 the beam disintegration after irradiation of the water filament with a focused IR laser pulse (see characteristics outlined above) is displayed in a series of micrographs recorded with a high-speed video stroboscope behind a microscope. The laser pulse is fired approximately at $t = 0$. As can be seen, the

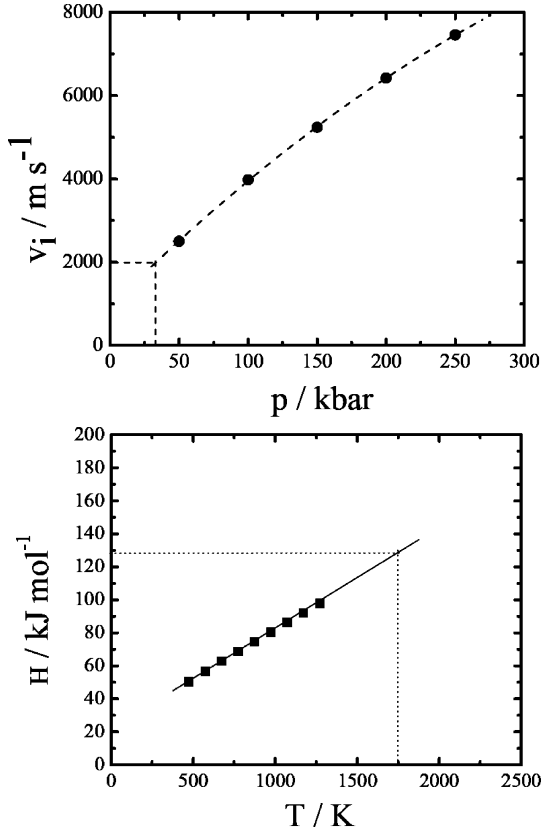

Figure 7. Upper panel: water/air interface velocity as a function of initial water (shock) pressure from ref 61 for the determination of the filament pressure in the present experiment. The dashed line is a fit through the data for extrapolation. Lower panel: high-enthalpy data from ref 63 for 30 kbar for filament temperature determination.

hot filament is nearly unchanged during the first 20 ns with a little bit of evaporation from the surface. The evaporation for the present conditions is difficult to estimate. Using the Hertz−Knudsen equation,[64,65] we found that for a temperature close to T_c, the evaporation diminishes the water beam within 20 ns diameter only by a few percent (∼5% at most). From the Figure 4 we conclude that evaporation is likely present already within the first 30 ns but it does not decrease the diameter significantly. It may, however, affect the surface temperature. The surface evaporation continues until the beam starts to disintegrate at $\Delta t = 30$ ns. This process is finished at about 50 ns; i.e., at that time it is completely exploded. Depending upon the energy content of the beam, this process may take 20 to 70 ns. From these data we conclude that the high-temperature filament exists for about 20−30 ns (for the high-temperature conditions this is an *upper limit*) and that the density of the hot (core of the) filament is probably still not very different from 1 g cm^{-3} during this time. Surface evaporation and very small volume expansions may also induce some time dependent radial temperature and pressure/density gradients in the filament. More information on this may be obtained from depth profiling measurements on the hot filament and reaction yields as a function of (ion gate) delay time Δt in the present experiment. In section D of the present chapter we will come back to this issue.

C. Laser Desorption of Ionic Aggregates: Protonation and Ejection from the Water Beam. In the present approach we make use of the fact that, in the explosive expansion of the microfilament ions, preformed ionic aggregates of neutrals such as educt and products or even reactive intermediates can be *isolated from the liquid phase* and detected with time-of-flight mass spectrometry. This technique is a special application of liquid beam desorption mass spectrometry.[26,31] As was shown in a recent article, the detection can be linear and quantitative.[31] In the positive ion mode mostly protonated or (if present) cationic species are detected. It should be noted that in high-temperature (as well as supercritical high-density) water the ion product of water is much larger than that at ambient temperatures, which likely enhances the above protonation process of kinetic species. A complete discussion of all mechanistic aspects of liquid beam ion mass spectrometry is certainly beyond the scope of the present article. For mechanistic details we refer the reader to ref 31 and a recent review.[66] It is important to realize that during the laser excitation of a few nanoseconds and the very fast vibrational energy relaxation the water filament does not evaporate immediately but heats significantly above its critical point (see previous section). After the laser-induced temperature jump and a lag-time of about 20−30 ns, an explosive expansion follows, which accelerates water vapor as well as protonated molecules or ions in free form or within water aggregates of various sizes ("nanodroplets"). In the explosive decay of the superheated beam, the high-temperature water reaction is efficiently quenched via expansion and evaporative cooling and reaction products in the form of completely desolvated ionic or protonated species or protonated clusters of various sizes are finally detected via mass spectrometry.[31]

For the experiment it is important to note that charge isolation from the high-density and high-temperature water phase can be due to two mechanisms depending upon the microenvironment of the ions or ionic aggregates. If the ions (ionic aggregates) are in the (supercritical) gas phase, only the small fraction that does not recombine is detected. This charging mechanism we will call *incomplete charge recombination* from the high-density gas phase. The cooling of the hot supersonic seeded gas jet may efficiently terminate (gas phase) chemical reactions beyond the beam disintegration time.[67,68] If we would assume that the micro water filament would be solely in the supercritical phase, we would have to assume a dense gas phase and the mechanism of *incomplete charge recombination* only. From our high-speed laser stroboscopy data we know that the laser-induced beam disintegration resembles rather a beam dispersion into small droplets than an evaporation and expansion of a supercritical gas phase. In addition, even if a supercritical gas phase is expanding at very short times ,droplets may be generated via fast recondensation after a very small volume release (expansion) of the hot filament. So, we assume that to a large extent very small droplets in the nanometer range are formed. These hot droplets may evaporate and pass the charge to the embedded molecule[31] a mechanism that resembles the classic *charge residue model*.[69] The charges on the droplets, in general, may have different origins; however, for the present conditions we have discussed the charging mechanism in some detail in a recent paper.[31] If the liquid is dispersed into droplets or spheres (with embedded ion) that are smaller than the Debye screening radius, there is a high probability for obtaining charged spheres or aggregates (microsolvated molecules). The latter appears to be closely linked to the appearance of (low) charge states in the experiment.[31] The heat of evaporation of water is ∼40 kJ/mol, and the molar heat capacity of water is on the order of 75 J/(mol K). For evaporation of an isolated droplet in a vacuum that is still liquid, the evaporation energy can only come from the internal energy of the droplet. The result is that evaporative cooling is enormously efficient—evaporation of half of a droplet cools the remaining half by about 500 K. Another consequence of this fact is that initial droplet temperature must

be well above 1000 K for complete evaporation. The time scale of the complete cooling process is on the order of microseconds, which implies very large cooling rates.

Due to these features we have a microreactor of superheated water that lasts for about 20−30 ns and in which chemical reactions can take place. After the reaction time that is determined by the system and laser parameters, the microbeam disintegrates and educt as well as product molecules are released either in the gas phase or in nanodroplets. Due to *incomplete ion recombination*[26,30] or charging due to the *charge residue (droplet) model*[69,70] educts, products, as well as intermediates (often in the form of their protonated adducts), can be detected in a quantitative fashion with time-of-flight-mass spectrometry.

D. Reaction Products of Resorcinol in Superheated and High-Density Water. For first exploratory experiments of chemistry in ultrahigh-temperature, -pressure and -density water we have chosen resorcinol as a benchmark system because it is well studied in high-temperature and supercritical water environments. At the same time its structure and chemistry is still simple enough to understand in a complex combustion type experiment like the present one. Typical reactions under less extreme SC water conditions and at lower densities are oxidation and radical reactions (see ref 14). At the high densities of water in our experiment it may be anticipated that the ionic reaction channel may compete against radical reactions. The increased stabilization of ions is indeed reflected in the dramatically increased ion product of water as opposed to low-density SC water, which by itself may already catalyze certain reactions that would not be the case under normal or less extreme conditions. It is the advantage of the present approach that it would be able to detect ionic intermediates in the high-enthalpy phase via laser desorption mass spectrometry if they are present.

A typical mass spectrum of the experiment under the conditions outlined in the previous chapter is displayed in Figure 8 (upper panel). The spectrum is obtained from a series of added spectra at different delay (ion gate) times Δt, when Δt is scanned between 6 and 12 μs. The summed spectrum rather than the gated spectra provides information about overall products and relative yields. What appears to be a disadvantage at first sight is actually a nice analytic tool because features of the explosion and desorption process are projected onto the delay or gate times. This is why smaller masses from smaller aggregates (from lower density near surface regions of the filament) tend to appear at lower delay times and larger masses from larger aggregates (from the inner part of the filament) at larger Δt, respectively.

In Figure 8 the areas between the dotted lines give the sensitivity for the mass ranges at different gate times. This "mass effect" is not due to electric fields because the space between the beam and the gated ion optics is field-free. Instead, the aggregates stem from slightly different locations in the hot disintegrating beam and have experienced slightly different environments, a feature that may be valuable in providing depth profiling information. We will come back to this feature below. It is important to note that under the present extreme conditions no larger fragmentation occurs, which would be visible at lower masses, and no multiaromatic ring products[14] are observed.

In the lower panel of Figure 8 an enlarged portion of the mass spectrum is displayed with mass assignments. It should be pointed out that the charge state in this type of experiment is usually +1 only (singly protonated species MH^+) and the mass resolution $m/\Delta m$ is on the order of 500−1000, making mass assignments relatively easy and straightforward. For the following mass peak assignments we refer to Scheme 1 in which the structures of the educt and several products observed as

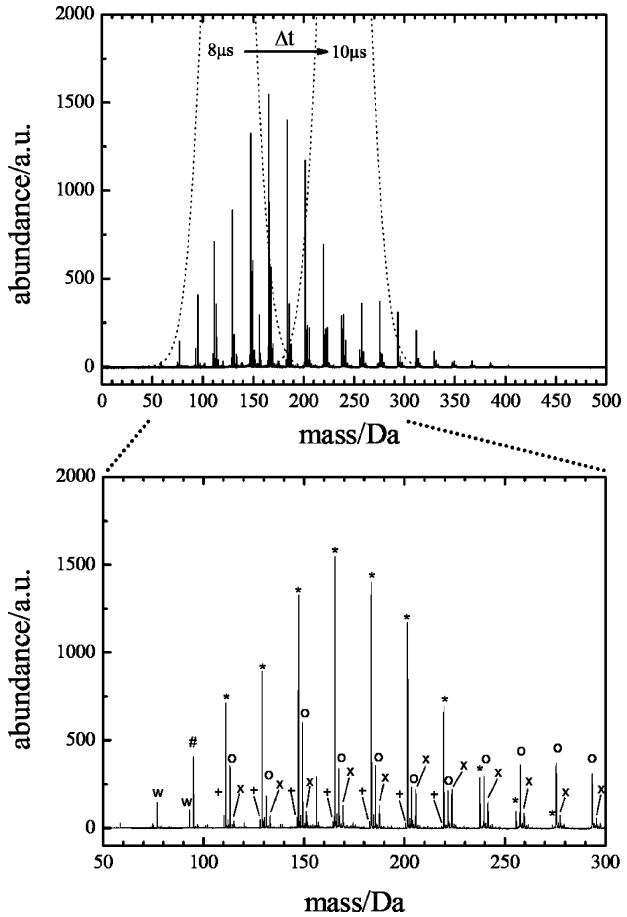

Figure 8. Mass spectrum of the educt (in the form of protonated resorcinol and resorcinol−water clusters) and protonated (microsolvated) reaction products. Upper panel: overview spectrum obtained by summation of different spectra at different delay times Δt (see Figure 1). For a given delay different portions of the spectrum are sampled (•••) that are added when Δt is scanned. Lower panel: enlarged portion of the spectrum between 50 and 300 Da. The peaks labeled by *, ○, ×, and + correspond to the progression of singly protonated aggregates (resorcinol) + nH$_2$O, (a) + nH$_2$O, (b) + nH$_2$O, and (c) + nH$_2$O (progression starts with the desolvated protonated species) with masses (110 + n18 + 1) Da, (112 + n18 + 1) Da, (114 + n18 + 1) Da, and (110 + n18) Da, respectively (for assignments see also Scheme 1). #: phenol. W: residual water lines. The spectrum is obtained by scanning Δt in the experiment and by adding all spectra obtained at different delay times (6−12 μs).

protonated species or protonated water adducts are shown. The masses labeling the structures therefore give the mass of the product and the mass of the protonated species (in parentheses) as observed in the experiment.

Note that all neutrals can only be observed as protonated adducts or protonated water aggregates. It was anticipated that resorcinol is desorbed from the water beam with more or less water attached, resulting in a large progression starting at mass 110(+1) Da. This has been observed in mild IR/UV desorption experiments by Kondow and co-workers.[71] In the present experiment we obtain a somewhat more complex spectrum. Many lines that resemble the progression of the parent resorcinol have a multiplet structure (three stronger lines of variable intensity) with a spacing of two mass units. In addition, mass peaks below 110 Da are visible, possibly suggesting fragmentation. Such a pattern is obviously the signature of high-temperature water chemistry and has not been observed in ref 71 for milder desorption conditions and with UV postdesorption ionization. The peaks in Figure 8 labeled by a star (*) correspond to the progression (separated by 18 Da) of the singly protonated

SCHEME 1: Different High-Temperature Reaction Products of Resorcinol (Consistent with the Observed Mass Spectra) Generated on a Short Nanosecond Time Scale before Beam Disintegration[a]

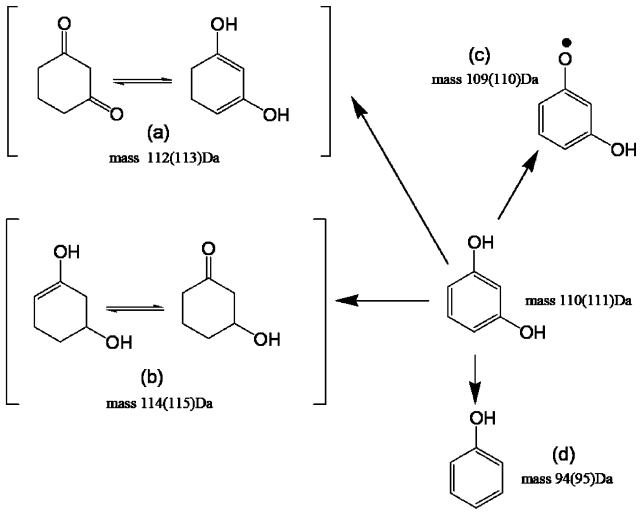

[a] The given masses correspond to the masses of the neutral species and the masses in brackets are those of the (detected) protonated aggregates (MH^+).

resorcinol + $n$$H_2O$ aggregates starting with the protonated parent molecule at mass 111 Da. The open circles (○) mark peaks of the (a) + $n$$H_2O$ progression resulting from the protonated product (a) displayed in Scheme 1 and its water adducts. The cross (×) labels the progression of the second (protonated) product (b) and protonated (b) + $n$$H_2O$ aggregates. A third low-abundance product (+) has a similar signature and a progression resulting from (c) + H^+ and protonated (c) + $n$$H_2O$ aggregates. The corresponding masses are (110 + n18 + 1) Da, (112 + n18 + 1) Da, (114 + n18 + 1) Da, and (110 + n18) Da, respectively (for assignments see also Scheme 1). Below 110 Da a phenol peak (#) belonging to product d in Scheme 1 and residual water lines (W) have been found.

In summary, beyond the parent resorcinol and a small yield of a species with a mass of 110−1 Da, which we attribute to the radical c in Scheme 1, we find two hydration products, (a) and (b), of resorcinol, which is surprising at first glance. The main product in our hot water filament is obviously the hydrated resorcinol (a), as observed from the intensities of the corresponding mass peaks (small contributions from protonated phenol−water aggregates appearing at masses (113 + n18)Da cause a slight overestimation of the yield for lower masses). Contrary to oxidation reactions usually present under less extreme and dense supercritical conditions, we observe hydration and little H-atom abstraction during the narrow time window of the experiment. Small amounts of radicals (c) but no ionic intermediates other than simple proton adducts are detected. These protonated adducts are likely not reaction intermediates but simple unspecific complexes.

Still the experimental finding is somewhat unexpected. Under the extreme temperature and high-density conditions obviously the hydration (reduction) of resorcinol is more favorable than oxidation reactions initiated by (OH) radical reactions. The experimental findings can be rationalized if the short time scale, the high-enthalpy environment, and the high density (1 g/cm^3) that is hardly possible in any other experiment are considered. Under the present conditions and on the relevant time scale most bimolecular reactions are diffusion limited and are usually too slow to contribute if the reactant is not in close contact with the embedded educt. This makes also secondary reaction steps

SCHEME 2: (A) Proposed Mechanism for a High-Temperature Hydration of Resorcinol in the Laser-Heated Water Filament and (B) Earlier and Later Fractions of Products after Filament Disintegration[a]

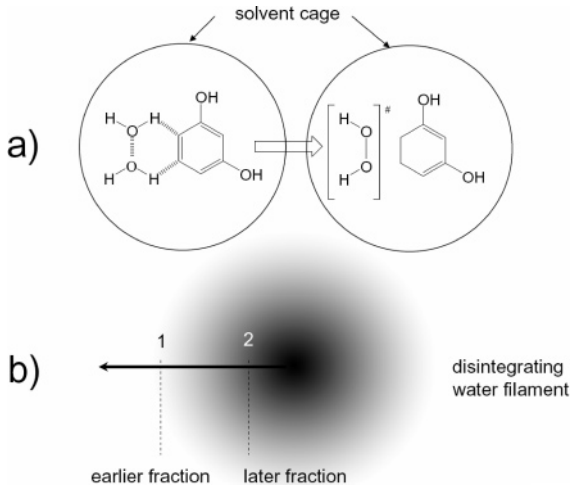

[a] For more details see the text.

highly unlikely. What is possible and remaining on the time scale of the experiment are fast unimolecular reactions of the resorcinol and fast bimolecular reactions with water, which is in close contact and part of the solvent cage around the reactant.

If OH radicals are generated under the present high-enthalpy conditions, they could initiate H-atom abstraction reactions but probably not complete oxidation chains including ring opening reactions. This primary H-atom abstraction reaction is seen to some extent in the experiment (product c). Hot resorcinol may undergo a fast unimolecular dissociation reaction, which may explain the formation of phenol on the fast time scales of the experiment. The yield of the unimolecular dissociation channel, however, is only moderate, which may be explained by a fast *in cage* recombination in the high-density environment leading back to the parent resorcinol. This behavior is not unexpected given the dense high-enthalpy environment and the short time scales, which are very different from other high-temperature water studies on this system. What is somewhat special for a high-enthalpy and high-density water environment are the observed hydration reactions leading to products a and b.

As depicted in Scheme 2a, a hydration reaction can only involve water as a reaction partner. Although water is not a typical hydration agent nor frequently actively involved in reduction reactions, its energy content in the high-temperature environment is large. The high energy content and the fact that there is not other reactant around have led us propose the "mechanism" depicted in Scheme 2a). A hydration may be possible if two water molecules are in close contact with each other and with the reactant, which may hydrate the aromatic ring of resorcinol and in turn form hydrogen peroxide. It is unclear at present whether this process is concerted or sequential or if it involves single water molecules (giving OH radicals that recombine to H_2O_2) or a special "transition state" as suggested in Scheme 2a). Hydrogen peroxide may boil off the cluster after reaction, dissociate to give two OH radicals (which may finally boil off) or stay in contact with the reaction product. In any case it is difficult to detect, because the protonated hydrogen peroxide−product a complex appears at the same mass as the resorcinol water clusters. A mass change (such as observed here) can only be observed if the H_2O_2 is boiled off the complex. Obviously, a double hydration is much less likely than the single process, which may be due to steric effects and the limited time

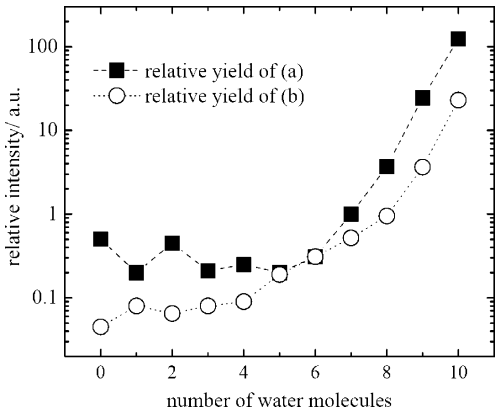

Figure 9. Relative yield (I_a/I_0 and I_b/I_0) of the reaction products (a) and (b) as a function of water molecules in the protonated aggregates. I_0 is the intensity of the protonated resorcinol−water aggregates at the corresponding masses ($110 + n18 + 1$) Da in the progression.

scale. However, following chemical intuition, the proposed reaction mechanism is difficult to prove and it is difficult to compare with similar experiments in the literature. However, the thermolysis of water at high temperatures to yield molecular hydrogen and oxygen (and reactive intermediates such as H, OH, and H_2O_2) is known to happen at very high temperatures, such as observed in high-temperature reactors in nuclear power plants.[72]

The chemical effect of ultrasound on aqueous solutions has been studied for many years. Primary products are often molecular hydrogen (H_2) and hydrogen peroxide (H_2O_2).[4] Other high-energy intermediates include HO_2 (superoxide), $H^{\bullet}$ (atomic hydrogen), and $OH^{\bullet}$ (hydroxyl). Interestingly, the sonolysis of water produces both strong reductants and oxidants responsible for primary and secondary oxidation and reduction reactions.[4]

The reduction reaction observed in the present study is most likely an effect of the high-enthalpy dense water environment. If the relative intensities of the mass peaks of products a and b are analyzed as a function of the number of water molecules in Figure 8, it is found that the relative yield increases with the increasing number of water molecules. In Figure 9 relative yields (I_a/I_0 and I_b/I_0) of the reaction products (a) and (b) are plotted as a function of water molecules in the protonated aggregates. I_0 is the intensity of the protonated resorcinol−water aggregates at the corresponding masses ($110 + n18 + 1$)Da in the progression. It is now important to note that the larger protonated water clusters stem preferentially from a later fraction of the explosion process, which is reflected by the larger delay or ion gate time Δt. According to Scheme 2b, this implies that the larger water clusters arriving later in the ion optics originate from the interior of the disintegrating beam and the fastest smaller aggregates from the outer spheres of the exploding beam. Consequently, the reaction yield in the larger water aggregates may be larger (likely due to the larger temperature, pressure, and density). This qualitative and certainly not sophisticated "depth profiling" of the reaction yield supports our previous mechanistic conclusions and may shed some light on the issue of radial inhomogeneities of the hot filament in the previous section). It will be further investigated in future experiments.

4. Summary and Conclusions

In summary, we have demonstrated that water at extreme temperature, pressure, and density can be generated via rapid laser heating. The determined experimental conditions (30 kbar, 1750 K, density ∼1 g/cm^3, energy content of water ∼130 kJ/mol) during the 20−30 ns lifetime of the water filament are indeed rather extreme and unique and provide an interesting environment for high-temperature water chemistry. In the disintegration of the superheated beam high-temperature water reactions are efficiently quenched via expansion and evaporative cooling and reaction products in the form of completely desolvated protonated species or protonated water clusters of various size are finally detected via time-of-flight mass spectrometry (TOF-MS). A decisive feature of the technique is that neutral products are detected as protonated aggregates.

For first exploratory experiments for chemistry in ultrahigh-temperature, -pressure and -density water, we have chosen resorcinol, a phenol derivative, as a benchmark system because it is well studied in high-temperature and supercritical water environments. A the same time its structure and chemistry is still simple enough to understand in a complex combustion type experiment like the present one. Contrary to oxidation reactions usually present under less extreme and dense supercritical conditions, we observe hydration and little H-atom abstraction during the narrow time window of the experiment. Small amounts of radicals but no ionic intermediates other than simple proton adducts are detected. The experimental findings are rationalized in terms of the energetic and dense environment and the short time scale of the experiment and provides firm evidence for new chemistry in extreme molecular environments.

In future experiments also mixtures will be investigated, e.g., supercritical water oxidation with added hydrogen peroxide, and high-energy compounds. The method appears to be well suited for fundamental reaction dynamics and kinetics in the condensed phase and in high-enthalpy and supercritical water or other solvents. The somewhat involved analysis of the high-enthalpy fluid's state (with what we call the *enthalpy method*) could be circumvented if an alternative method for a robust temperature determination could be used. In principle, the temperature dependence of a well-known reaction proceeding in parallel to the reactions to be studied may be exploited. Such a concept of a standard reaction and self-calibrating system is well-known for single shot combustion experiments in shock tubes.[73] Also the approach of using a "chemical thermometer" as reported in ref 6 is similar in spirit and appears promising in particular with an additional kinetic energy analysis.

Finally, it should be noted that also the detection of the neutral species (as neutrals) from the desorption process may be important for mechanistic studies. In such a case a soft UV ionization with a second laser such as developed by Baer and Miller[6] could be the method of choice. In addition to protonation at high temperatures, which is a quantitative and a powerful method of detecting a large range of species of very different proton affinities, negatively charged species and adducts (OH^-) can be detected as well in the negative ion mode of the spectrometer, making the detection scheme (with one IR desorption laser only) truly universal for product screening in laser-heated microfilaments.

Acknowledgment. This work was supported from the Deutsche Forschungsgemeinschaft (DFG) within the Sonderforschungsbereich 357 and the Graduiertenkolleg 782. Discussions of several aspects of the present work with Prof. Dr. J. Troe, Prof. Dr. M. Buback, and Prof. Dr. K. Luther, as well as valuable comments and suggestions of the referees are gratefully acknowledged.

References and Notes

(1) Manaa, M. R. *Chemistry at Extreme Conditions*; Elsevier Science: New York, 2005.

(2) Dressler, R. *Chemical dynamics in extreme environments*; World Scientific: New York, 2001.
(3) Didenko, Y. T.; Suslick, K. S. *Nature* **2002**, *418*, 394.
(4) Suslick, K. S. *Sci. Am.* **1989**, *2* (Feb), 80.
(5) Dlott, D. D. *Acc. Chem. Res.* **2000**, *33*, 37.
(6) Woods, E.; Miller, R. E.; Baer, T. *J. Phys. Chem. A* **2003**, *107*, 2119.
(7) Dessiaterik, Y.; Nguyen, T.; Baer, T.; Miller, R. E. *J. Phys. Chem. A* **2003**, *107*, 11245.
(8) Zelenyuk, A.; Cabalo, J.; Baer, T.; Miller, R. E. *Anal. Chem.* **1999**, *71*, 1802.
(9) DeForest, C. L.; Quian, J.; Miller, R. E. *Appl. Opt.* **2002**, *41*, 5804.
(10) Cabalo, J.; Zelenyuk, A.; Baer, T.; Miller, R. E. *Aerosol Sci. Technol.* **2000**, *33*, 3.
(11) Leitner, W. *Acc. Chem. Res.* **2002**, *35*, 746.
(12) Akiya, N.; Savage, P. E. *Chem. Rev.* **2002**, *102*, 2725.
(13) Katritzky, A. R.; Allin, S. M.; Siskin, M. *Acc. Chem. Res.* **1996**, *29*, 399.
(14) Savage, P. E. *Chem. Rev.* **1999**, *99*, 603.
(15) Watanabe, M.; Sato, T.; Inomata, H.; Smith, R. L.; Arai, K.; Kruse, A.; Dinjus, E. *Chem. Rev.* **2004**, *104*, 5803.
(16) Kajimoto, O. *Chem. Rev.* **1999**, *99*, 355.
(17) von Benten, R.; Charvat, A.; Link, O.; Abel, B.; Schwarzer, D. *Chem. Phys. Lett.* **2004**, *386*, 325.
(18) Baulch, D.; Cobos, C.; Cox, R.; Frank, P.; Hayman, G.; Just, T.; Kerr, J.; Murrells, T.; Pilling, M.; Troe, J.; Wlker, R.; Warnatz, J. *J. Phys. Chem. Ref. Data* **1994**, *23*, 487.
(19) Westacott, R. E.; Johnston, K. P.; Rossky, P. J. *J. Am. Chem. Soc.* **2001**, *123*, 1006.
(20) Westacott, R. E.; Johnston, K. P.; Rossky, P. J. *J. Phys. Chem. B* **2001**, *105*, 6611.
(21) Brill, T. B. *J. Phys. Chem. A* **2000**, *104*, 4343.
(22) Bell, W. C.; Boohsh, K. S.; Myrick, M. L. *Anal. Chem.* **1998**, *70*, 332.
(23) Myrick, M. L.; Kohs, J.; Parsons, E.; Chike, K.; Lovelace, M.; Scrivens, W.; Holliday, R.; Williams, M. J. *J. Raman Spectrosc.* **1994**, *25*, 59.
(24) Bennett, G.; Johnston, K. P. *J. Phys. Chem.* **1994**, *98*, 441.
(25) Terry, J. L.; Fox, M. A. *J. Phys. Chem. A* **1998**, *102*, 3705.
(26) Kleinekofort, W.; Avdiev, J.; Brutschy, B. *Int. J. Mass Spectrom. Ion Processes* **1996**, *152*, 135.
(27) Dreisewert, K. *Chem. Rev.* **2003**, *103*, 395.
(28) Faubel, M.; Kisters, T. *Nature* **1989**, *339*, 527.
(29) Charvat, A.; Lugovoj, E.; Faubel, M.; Abel, B. *Rev. Sci. Instrum.* **2004**, *75*, 1209.
(30) Charvat, A.; Lugovoj, E.; Faubel, M.; Abel, B. *Eur. Phys. J. D* **2002**, *20*, 573.
(31) Abel, B.; Charvat, A.; Diederichsen, U.; Faubel, M.; Girmann, B.; Niemeyer, J.; Zeeck, A. *Int. J. Mass Spectrosc.* **2005**, *243*, 177.
(32) Martino, C. J.; Savage, P. E. *Ind. Eng. Chem. Res.* **1997**, *36*, 1385.
(33) Martino, C. J.; Savage, P. E. *Ind. Eng. Chem. Res.* **1997**, *36*, 1391.
(34) Oshima, Y.; Hori, K.; Toda, M.; Chommanad, T.; Koda, S. *J. Supercrit. Fluids* **1998**, *13*, 241.
(35) Rice, S. F.; Steeper, R. R. *J. Hazard. Mater.* **1998**, *59*, 261.
(36) Thammanayakatip, C.; Oshima, Y.; Koda, S. *Ind. Eng. Chem. Res.* **1998**, *37*, 2061.
(37) Assmann, J.; Kling, M.; Abel, B. *Angew. Chem. Int. Ed.* **2003**, *42*, 2226.
(38) Nienhuis, H.-K.; Woutersen, S.; Santen, R. A.; Bakker, H. J. *J. Chem. Phys.* **1999**, *111*, 1494.
(39) Woutersen, S.; Emmerichs, U.; Bakker, H. J. *Science* **1997**, *278*, 658.
(40) Stasicki, B.; Charvat, A.; Faubel, M.; Abel, B. *Proc. SPIE* **2004**, *5580*, 335.
(41) Kritzer, P. *J. Supercrit. Fluids* **2004**, *29*, 1.
(42) Charvat, A.; Lugovoj, E.; Faubel, M.; Abel, B. *Rev. Sci. Instrum.* **2004**, *75*, 1209.
(43) Buck, U.; Steinbach, C. Vibrational Spectroscopy and Reactions of Water Clusters. In *Water in Confining Geometries*; Buch, V., Devlin, P., Eds.; Springer: Berlin, 2003; p 53.
(44) Kirmse, B.; Abel, B.; Schwarzer, D.; Grebenshchikov, S. Y.; Schinke, R. *J. Phys. Chem. A* **2000**, *104*, 10398.
(45) Wieliczka, D. M.; Weng, S.; Querry, M. R. *Appl. Opt.* **1989**, *28*, 1714.
(46) Vogel, A.; Venugopalan, V. *Chem. Rev.* **2003**, *103*, 577.
(47) Walrafen, G. E. Raman and Infrared spectral investigations of water structure. In *Water—A comprehensive treatise*; Francks, F., Ed.; Plenum Press: New York, 1976; Vol. 1, p 151.
(48) Kiang, Y. C.; Lang, R. W. *Appl. Opt.* **1983**, *22*, 1296.
(49) Siegman, A. E.; Sasnett, M. W.; Johnston, J., T. F. *IEEE J. Quantum Electron.* **1991**, *27*, 1098.
(50) Kerker, M. *The Scattering of Light and Other Electromagnetic Radiation*; Academic: New York, 1969.
(51) Kuboda, N. *Propellants and Explosives*; Wiley-VCH: Weinheim, 2002.
(52) *CRC Hanbook of Chemistry and Physics*, 63rd ed.; Weast, R. C., Astle, M. J., Eds.; CRC Press: Boca Raton, FL, 1982.
(53) Wiryana, S.; Slutsky, L. J.; Brown, J. M. *Earth Planet. Sci. Lett.* **1998**, *163*, 123.
(54) Paltauf, G.; Dyer, P. E. *Chem. Rev.* **2003**, *103*, 487.
(55) Cowperthwaite, M.; Shaw, R. *J. Chem. Phys.* **1970**, *53*, 555.
(56) Gurtman, G. A.; Kirsch, J. W.; Hastings, C. R. *J. Appl. Phys.* **1971**, *42*, 851.
(57) Mitchell, A. C.; Nellis, W. J. *J. Chem. Phys.* **1982**, *76*, 6273.
(58) Zel'dovich, Y. B.; Kormer, S. B.; Sinitsyn, M. V.; Yushko, K. B. *Sov. Phys. Dokl.* **1961**, *6*, 494.
(59) Chazaud, F.; Sentis, M. L.; Le, H. C.; Rigneault, H.; Delaporte, P., C. *Appl. Phys. Lett.* **1994**, *65*, 1626.
(60) Kim, J. U.; Lee, H. J.; Kim, C.; Kim, G. H.; Suk, H. *J. Appl. Phys.* **2003**, *94*, 5497.
(61) Rice, M. H.; Walsh, J. M. *J. Chem. Phys.* **1957**, *26*, 824.
(62) Zel'dovich, Y. B.; Raizer, Y. P. *Sov. Phys. JETP* **1959**, *8*, 980.
(63) Tödheide, K. Water at high temperatures and pressures. In *Water—A comprehensive treatise*; Francks, F., Ed.; Plenum Press: New York, 1976; Vol. 1, p 463.
(64) Kelly, R. *J. Chem. Phys.* **1990**, *92*, 5047.
(65) Kelly, R.; Miotello, A. *Nucl. Instrum. Methods Phys. Res. B* **1997**, *122*, 374.
(66) Charvat, A.; Boegehold, A.; Abel, B. *Aust. J. Chem.*, in press.
(67) Fenn, J. In *Applied Atomic Collision Physics*; Academic Press: New York, 1982; Vol. 5, p 349.
(68) Williams, P.; Nelson, R. W. On the mechanism of volatilization of large biomolecules by pulsed laser ablation of frozen aqueous solution. In *Methods and mechanisms for producing ions from large molecules*; Standing, K. G., Ens, W., Eds.; Plenum Press: New York, 1991.
(69) Dodd, E. E. *J. Appl. Phys.* **1953**, *24*, 73.
(70) Schmelzeisen-Redeker, G.; Bütfering, L.; Röllgen, F. W. *Int. J. Mass Spctrom. Ion Processes* **1989**, *90*, 139.
(71) Horimoto, N.; Kohno, J.; Mafune, F.; Kondow, T. *J. Phys. Chem. A* **1999**, *103*, 9569.
(72) Schultz, K. R.; Brown, L. C.; Besenbruch, G. E.; Hamilton, C. J. *Large-scale production of hydrogen by nuclear energy for the hydrogen economy*; General Atomics Report GA-A24265; 2003.
(73) Meyer, E.; Olschewski, H. A.; Troe, J.; Wagner, H. G. *XII. International Symposium on Combustion*; The Combustion Institute: Pittsburgh, PA, 1969; p 345.